New Development in Understanding Drug-Polymer Interactions in Pharmaceutical Amorphous Solid Dispersions from Solid-State Nuclear Magnetic Resonance

Andrea Pugliese[a], Michael Tobyn[b], Lucy E. Hawarden[b], Anuji Abraham[c], and Frédéric Blanc[a,d,*]

[a] Department of Chemistry, University of Liverpool, Liverpool L69 7ZD, United Kingdom

[b] Drug Product Development, Bristol-Myers Squibb, Moreton CH46 1QW, United Kingdom

[c] Drug Product Development, Bristol-Myers Squibb, New Brunswick, New Jersey 08903, United States

[d] Stephenson Institute for Renewable Energy, University of Liverpool, Liverpool L69 7ZF, United Kingdom

* To whom correspondence should be addressed: frederic.blanc@liverpool.ac.uk

Abstract

Pharmaceutical amorphous solid dispersions (ASDs) represent a widely used technology to increase the bioavailability of active pharmaceutical ingredients (APIs). ASDs are based on an amorphous API dispersed in a polymer, and their stability is driven by the presence of strong intermolecular interactions between these two species (*e.g.*, hydrogen bond, electrostatic interactions, etc.). The understanding of these interactions at the atomic level is therefore crucial, and solid-state nuclear magnetic resonance (NMR) has demonstrated itself as a very powerful technique for probing API-polymer interactions. Other reviews have also been published reporting exciting approaches to study the structures and dynamic properties of ASDs and largely focusing on the study of API-polymer miscibility, and on the identification of API-polymer interactions. Considering the increased use of NMR in the field, the aim of this review is to specifically highlight recent experimental strategies used to identify API-polymer interactions reporting promising recent examples using one-dimensional (1D) and two-dimensional (2D) experiments by exploiting the following emerging approaches of very-high magnetic field and ultra-fast magic angle spinning (MAS). A range of different ASDs spanning APIs and polymers with varied structural motifs is targeted to illustrate new ways to understand the mechanism of stability of ASDs enabling the design of new dispersions.

Keywords

Amorphous solid dispersions (ASDs), solid state nuclear magnetic resonance (NMR), API-polymer interactions, ASD stability, hot-melt extrusions (HME), spray-drying (SD).

TOC

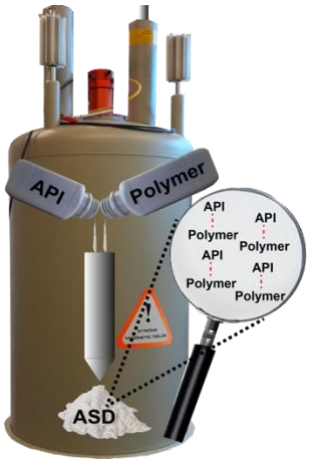

1. Amorphous Solid Dispersions

The formulation of low solubility crystalline active pharmaceutical ingredients (APIs) or drugs in the amorphous form is a recognised robust methodology exploited to improve their dissolution rates and bioavailability.[1,2] ASD's can be used for other purposes, such as the enhancement of stability when salt forms of an API are unstable. Several approaches have been developed to stabilise amorphous solid dispersions (ASDs) among which hot-melt extrusion (HME) and spray-drying (SD) technologies are the most widely used, and the only ones used commercially by the pharmaceutical industry.[3-5] ASDs are formulations of one (or more) active ingredient in the amorphous state stabilised by inert and hydrophilic carrier(s) or matrix in the solid state (usually a polymer and/or additive) aimed at obtaining fully miscible, amorphous and physically stable dispersion.[6,7]

HME is utilised extensively for commercial-scale ASDs manufacturing because of several factors: it is mature, well understood process and can be therefore scalable and low cost; it is solvent free and thus environmentally friendly and it operates as a continuous process well suited for large scale production.[2,8] This technology contains several steps as illustrated in Figure 1(a) in which the drug and the polymer are mixed, melted, dispersed and extruded under specific conditions offering flexibility to be tailored to a range of API, matrix and other excipients while also being suitable to oxygen sensitive and hydrolysable drugs.[3] Two of the most important drawbacks of this technology are the high energy consumption of the process and heating processes preclude the formulation of thermolabile API's.[5]

Another widely used technology for commercially manufacturing ASDs in the pharmaceutical industry is spray-drying (SD) methodology that also offers a scalable process, albeit that scaling up is more complex than with HME.[4] The SD process (Figure 1(b)) requires an initial API-polymer solution/suspension in a system which might contain water as the feed solution which is then spray dried through a spray-nozzle (component 1 in Figure 1(b)) for which various design exists (components 2 – 4 in Figure 1(b)) to accommodate more than one feed or high-pressure.[5] Upon contact of the feed solution droplets with the hot gas/air carrier, the solvent system evaporates quickly leading to dried ASD particles that are separated by the gas stream in the cyclone and then collected. It is likely that the particles, once gathered, are subjected to a secondary drying process to remove solvents and reduce any residual moisture to an appropriate level. The spray dried systems can then be formulated into a conventional tablet system.

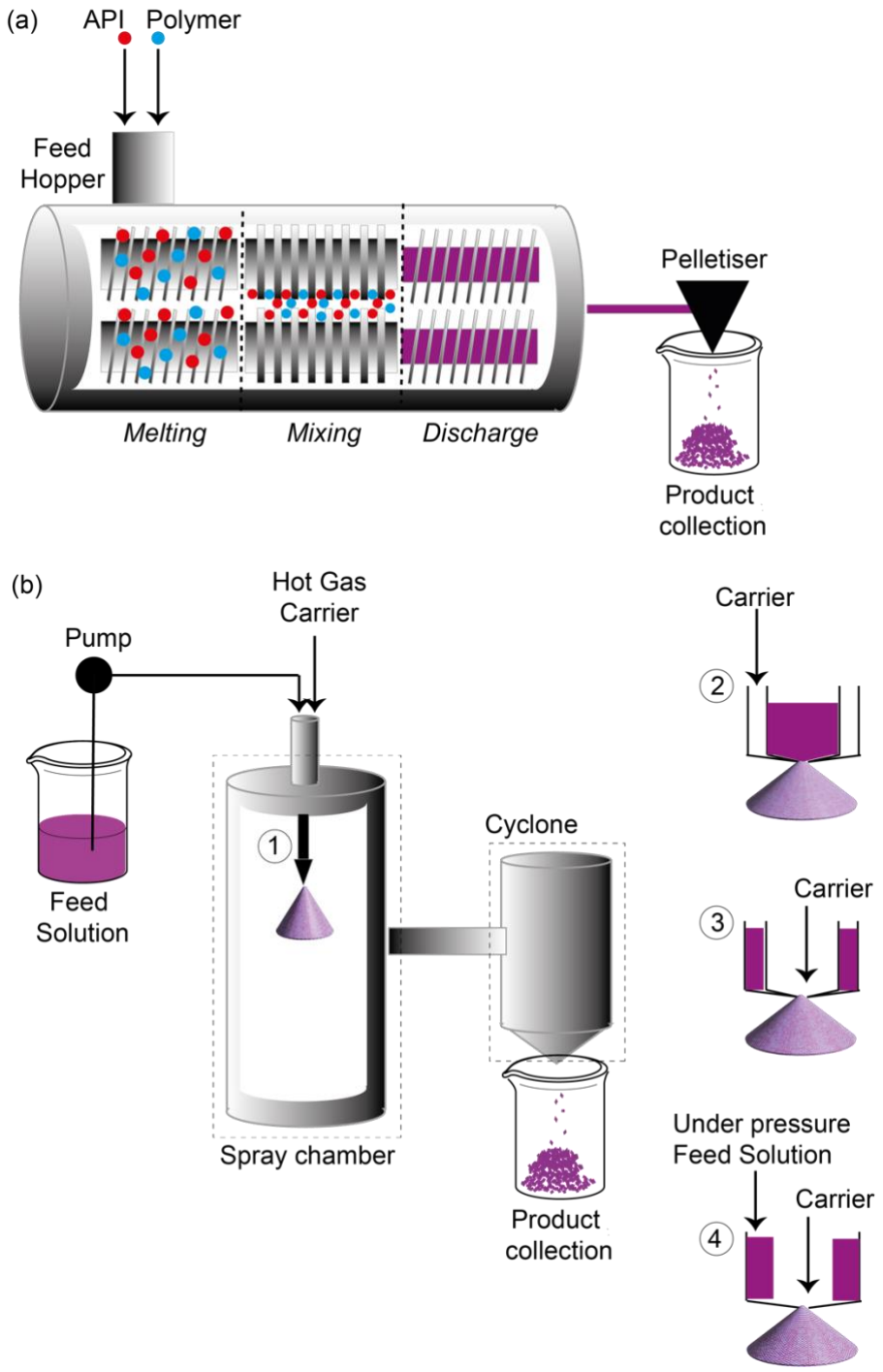

Figure 1. Schematics of (a) HME and (b) SD technologies for the preparation of ASDs. In (a), the three main steps are melting, mixing, and discharge where the material cools down and leaves the apparatus. Physical-chemical properties of the final product can be tuneable using different screws design and speed and controlling the temperature. In (b), the spray nozzle (component 1) of the chamber is available in several designs (components 2 – 4) based on the required specific applications. Figure adapted with permission from[5]. Copyright Elsevier (2021).

Polymers in ASDs play a key role in stabilising the thermodynamically metastable nature of the amorphous API. Polymers raise the inherent glass transition temperature (Tg) of the system, which effectively reduces the amorphous molecule's mobility, making it less likely that it will encounter other molecules to trigger the crystallization process. Further amorphous stability enhancement can be achieved by the existence of specific chemical interaction between the drug and API species to further reduce molecular mobility of the amorphous drug, and increase the Tg of the formulation.[9] The formation of drug-polymer intermolecular interactions, such as hydrogen bonding (H-bond), ionic forces, π−π, or electrostatic interactions, are well established as the most significant interactions capable of stabilising dispersed systems[8] by inhibiting recrystallization phenomena in the amorphous matrix and preventing competitive API−API or polymer−polymer intramolecular interactions. The identification and the understanding of the physical stability of ASDs remain a significant challenge and opens exciting future prospective designing ASDs stabilised by suitable and tuneable API-polymer interactions.[10]

Historically, thermal analysis methods, such as differential scanning calorimetry (DSC) and temperature-modulated DSC, have often been employed to elucidate API-polymer interactions in ASDs, allowing Tg measurements from which miscibility of the various ASD components can be inferred from.[11,12] One such approach is the Gordon−Taylor model[13] that estimates the Tg of an ideal binary mixture (Tg_{mix}), where significant deviations between the predicted Tg_{mix} and experimentally determined Tg provide useful information about interactions between the various constituents of the mixture, and potentially repulsive interactions which destabilise the system.[14,15]

A range of analytical methods including vibrational, Raman, and Fourier-transform infrared (FT-IR) spectroscopies have been used to provide atomic scale information about solid dispersions. Raman applications specifically include the measurements of crystallization rate,[16] while confocal Raman microscopy and Raman imaging have been employed in mapping solid dispersions to identify and discriminate crystalline/amorphous domains[17] thereby providing indirect information about the existence of API-polymer interactions. Evidence of recrystallization phenomena can be observed from changes in band wavelength and comparison of bands intensity ratio or from the study of spatially time-resolved Raman generated using multivariate curve resolution that leads to monitor the evolution of an amorphous drug in ASD. FT-IR methods probe H-bond in specific functional groups such as hydroxyl, amino, and carbonyl groups and permit identification of this specific interaction in the API and/or the polymer.[18] It has been shown that when those functional groups are involved in H-bond interactions, a simultaneous decrease in the stretching frequency and a

widening of their absorption bands are observed due to smaller intermolecular distances between the donor−acceptor groups.[19]

The wide use of these techniques is justified by their versatility (obtaining information on the internal energy of the samples, API-polymer miscibility, and the presence of molecular interactions), the small amount of sample required, ease of use, and relatively short analysis time. However, some drawbacks exist and include the presence of moisture for FT-IR data, the photodegradation of the sample in Raman spectroscopy, or by the experimental conditions (DSC and modulated DSC) which require careful consideration.

Solid-state Nuclear Magnetic Resonance (NMR) has emerged as a significantly powerful tool for accessing structural and dynamics information across the biological, chemical, material and physical sciences.[20,21] In particular, despite the high cost of the equipment, NMR is arguably the most powerful approach to obtain structural information at the atomic level and is complementary to the analytical techniques mentioned above. NMR plays an important role in pharmaceutical sciences[22,23] to enable structural understanding of API[24] and polymer[25,26], identify crystalline polymorphs[27], monitor drug recrystallization phenomena from amorphous systems, and understand API-polymer interactions in ASDs.[28-38] Although a number of reviews has been published on these topics, these papers report either broad overviews[39-41], or specific applications in the field (*e.g.*, ^{19}F).[42] This review aims at describing the use of solid-state NMR to the understanding of the stability of ASDs based on the presence of API-polymer interactions, and highlights the most modern NMR methodologies to achieving this. The purpose of this review is to discuss the recent exciting literature in the field while the interested readers are referred to several excellent monographs for the basics of NMR[43-46] and in the solid-state.[20,47,48] This review specifically reports on experimental NMR approaches to identify the presence of inter and intramolecular API-polymer interactions in ASDs prepared by HME or SD technologies with examples based on a range of structurally different drugs and polymers.

We first show that one-dimensional (1D) experiments can be employed to highlight the presence of API-polymer interactions based on changes in chemical shifts for certain signal(s) in the spectra of the ASD compared with those of the amorphous API or polymer. 1D experiments are also useful to identity API recrystallization processes from line shape analysis and relaxation measurements. We then reveal that the nature of the API-polymer interactions can be obtained from two-dimensional (2D) homo- and hetero-nuclear NMR correlations. In particular, we exemplify ^{1}H-^{13}C/^{19}F heteronuclear correlation (HETCOR) and ^{1}H-^{1}H dipolar double quantum (DQ) correlation as experiments identifying site-specific intermolecular contacts between API and polymer. Finally, we illustrate how 2D experiment carried out at

ultra-fast magic angle spinning (MAS) frequency (> 60 kHz) and very-high magnetic field (> 600 MHz, 14.1 T) and involving quadrupolar and/or low gyromagnetic nuclei (*i.e.* ^{14}N) can be used to probe API-polymer interactions.

2. Chemical shift as a unique observable of API-polymer interaction

The most straightforward experimental approaches currently used to characterise novel ASDs often include 1D NMR spectra data collection involving most, if not all, NMR active isotopes. This is accomplished from typically recording ^{1}H, ^{19}F, ^{13}C and ^{15}N NMR nuclei (as applicable) in which the chemical shielding interactions have been demonstrated to be very sensitive to subtle changes in local electronic environment, indicating the presence of API-polymer interactions in ASDs.

Solid-state NMR spectroscopy deals with powder samples consisting of many crystallites randomly oriented, hence the nuclear spin interactions such as chemical shielding, dipole-dipole coupling, and in cases involving nuclear spin larger than 1/2 (*e.g.*, ^{14}N), quadrupolar coupling, are all orientation dependent (or anisotropic). This results in a range of resonance frequencies leading to NMR signal broadening.[20,47] These anisotropic interactions can be successfully average out by magic angle spinning (MAS), in which the sample is spun at an angle of 54.7° (magic angle) with respect the direction of static magnetic field. Under conditions where the MAS frequency is in the same order of magnitude (or greater) than the NMR interactions, the broadened resonances observed in static (non spinning) solid-state NMR spectra largely vanish to yield narrower lines.

The direct observation of ^{1}H and ^{19}F NMR signals have been used to detect polymorphs in crystalline samples, to distinguish multiple APIs in ASDs, and have allowed the identification of molecular interactions between various components of the dispersion from chemical shift changes.[8,39] In addition, in 1D experiments, comparison of linewidths can be used to discriminate crystalline API from amorphous API as the latter experiences severe inhomogeneous line broadening arising from a large distribution of chemical environments randomly distributed[39,49], an effect that is not averaged out by MAS. The low receptivity of ^{13}C and ^{15}N arising from both low natural abundance (1.1 and 0.4%, respectively) and poor intrinsic sensitivity can significantly be overcome by the transfer of polarisation from highly receptive nuclei (usually ^{1}H or ^{19}F). In the solid state, this now routine approach is called cross polarisation (CP) in which the polarisation transfer is radio frequency driven by heteronuclear dipolar coupling.[48] This allows for spectra with higher signal-to-noise ratios to be obtained in a reasonable amount of experimental time (hours) for most ASDs even at relatively high API loading.

Figure 2 shows 1D ^{13}C and ^{15}N CP spectra that were successfully exploited to highlight H-bond interactions in ASDs between ketoconazole (KTZ) and a range of different polymers (such as poly(acrylic acid) (PAA), poly(2-hydroxyethylmethacrylate) (PHEMA) and polyvinylpyrrolidone (PVP)) with API concentration ranging between 4 and 12 wt %.[28] The ^{13}C CP MAS spectrum (Figure 2(a)) of the KTZ-PAA ASD reveals that the ***C***OOH signal of PAA experiences a change of shift to lower frequency relative to the physical mixture and PAA itself, that can be attributed to the disruption of the dimeric H-bond of PAA, hence indicating that the ***C***OOH is involved in stabilising the amorphous API. The ^{15}N CP MAS spectra of KTZ-PAA ASDs at different PAA loading (Figure 2(b)) show the existence of two N3 imidazole nitrogen signals at around 260 and 240 ppm that can be attributed to "free" KTZ and to a N3 engaged in an H-bond, respectively, as this 20 ppm change in shift is typical of H-bond interactions and supports that the most basic imidazole N3 nitrogen is engaged in stabilising the KTZ.[50] No changes in ^{15}N chemical shift is observed for the other imidazole nitrogen N1 signal or the piperazine nitrogens highlighting that the KTZ-PAA H-bond interactions occur exclusively between the most basic imidazole N3 nitrogen and the ***C***OOH PAA.

While no changes in ^{13}C chemical shift are observed between KTZ, KTZ-PHEMA ASD and physical mixture (Figure 2(c)), the ^{15}N chemical shift of the N3 nitrogen KTZ in KTZ-PHEMA ASD is observed at a lower frequency than in KTZ itself and indicates that this site is involved in the formation of API-polymer interaction likely with the -OH group of PHEMA.

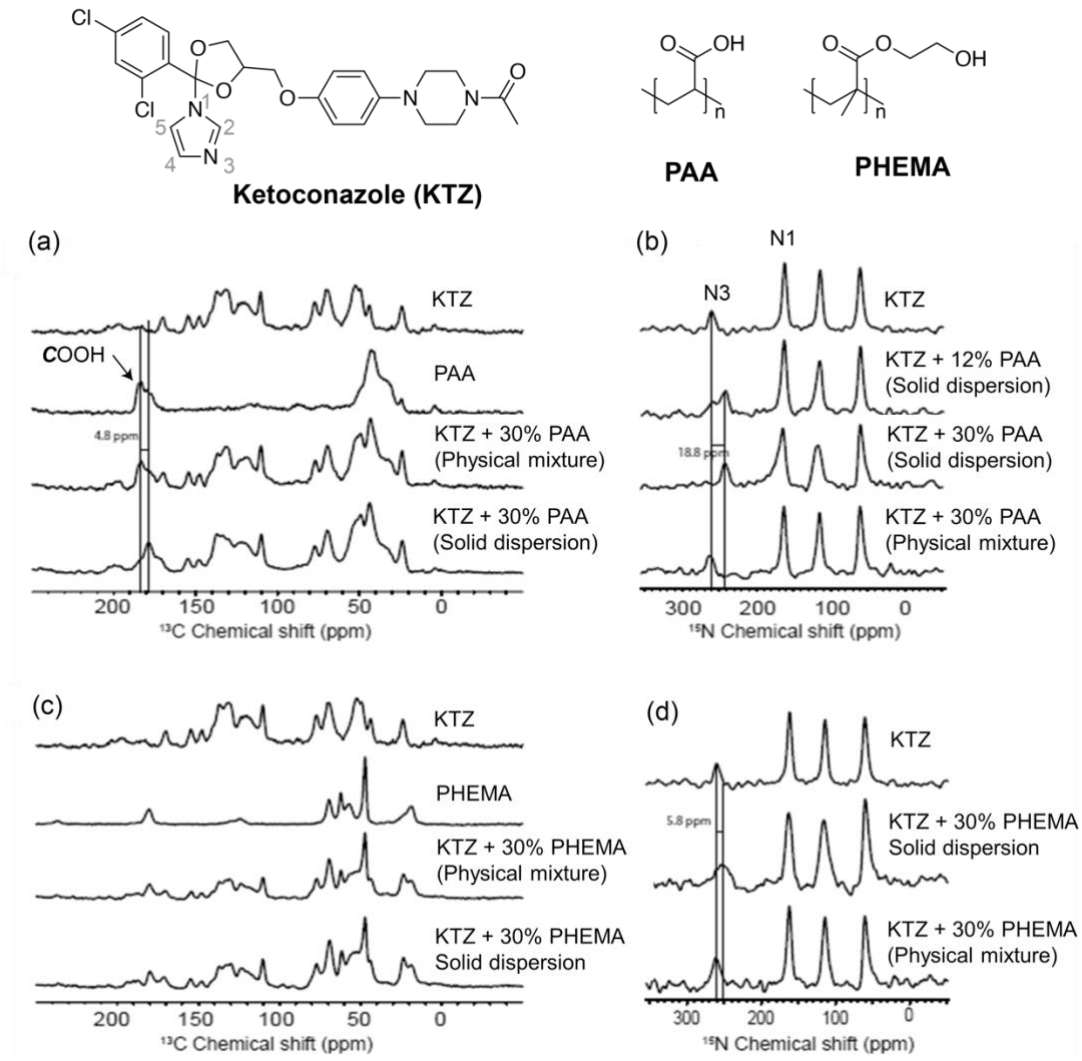

Figure 2. Comparison of the (a,c) ^{13}C and (b,d) ^{15}N CP MAS NMR spectra of amorphous KTZ, PAA and PHEMA polymers, their physical mixtures and ASDs. The vertical black lines highlight differences in chemical shifts in the ASDs with respect the individual components, indicating the presence of API-polymer interactions. The chemical structures of KTZ and polymers are shown on the top of the figure. Reprinted with permission from[28]. Copyright 2015 American Chemical Society.

Recently, a new class of ASDs has emerged, where a second polymer is added to the formulation. The capability of NMR to characterise this complex ternary ASD has been demonstrated using KTZ-HPMC-PAA ASD.[51] While no changes in chemical shift were highlighted in the ^{13}C spectra for the binary system KTZ-HPMC ASDs (Figure 3(a)) and excluded the possibility of interaction between the compounds, ^{13}C spectroscopic data for both KTZ-PAA and KTZ-HPMC-PAA dispersions (Figure 3(b) and (c)) showed some interesting similar spectral features. In both systems, the intensity of the peak corresponding to the PAA dimer form (at 182 ppm) decreases with respect to the free form (at 177 ppm), changes

intensity across the drug loading and, interestingly, a new peak at 172 ppm emerges corresponding to hydrogen bonded KET. Changes in chemical shift have been also highlighted in the ^{15}N spectra for both the binary KTZ-PAA and the ternary KTZ-HPMC-PAA ASDs (Figure 3(d)), suggesting of a proton transfer or salt formation.[32] These results probe the presence of ionic and H-bond interactions both in binary KTZ-PAA and ternary KTZ-PAA-HPMC ASDs, supported respectively, by the loss of PAA dimers resulting from the KTZ-PAA interaction and by the presence of the signal at 172 ppm that indicate the presence of hydrogen bonded KET

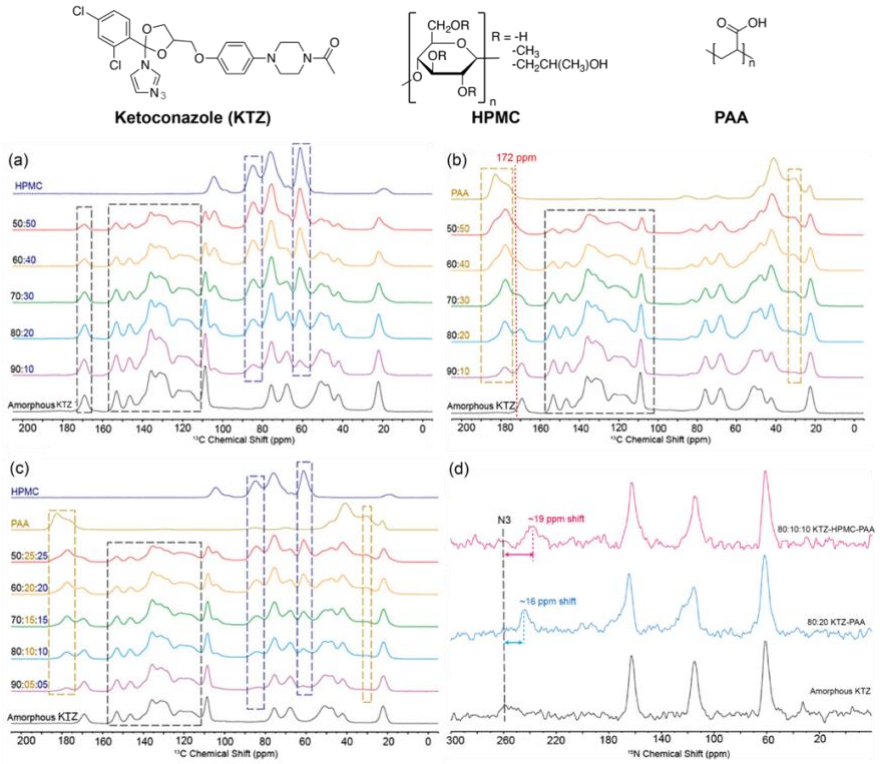

Figure 3. ^{13}C CP MAS spectra of (a) KTZ-HPMC, (b) KTZ-PAA, and (c) KTZ-HPMC-PAA ASDs at different drug loadings. (d) ^{15}N CP MAS spectra of amorphous KZT, KTZ-PAA, and the ternary KTZ-HPMC-PAA ASDs. Chemical structure of KET, HPMC, and PAA are given on the top of the figure. Reprinted with permission from[51]. Copyright 2020 American Chemical Society.

Acid-base interactions are also known to contribute significantly to API stabilisation in ASDs and are often much stronger than H-bonds, therefore offering exciting opportunities and attracting significant interests. However, only few acidic polymers in the pharmaceutical armoury are known and include PAA, hydroxypropylmethylcellulose (HPMC), hydroxypropylmethylcellulose acetate succinate (HPMC-AS) and poly(methacrylic acid-co-ethyl acrylate). These are, however, weakly acidic and not prone to protonate weakly basic moieties in APIs.

Polystyrene sulfonic acid (PSSA) polymer, which is currently not a pharmaceutically approved polymer, turned out as a promising inhibiter of re-crystallization for several APIs in ASDs by forming strong acid-base interactions.[52] Given that both lapatinib (LB) and gefitinib (GB) contain a range of basic nitrogen containing moieties such as anilinoquinazoline and amino groups, ^{15}N NMR spectroscopy has revealed itself to enable identification of their acid-base interactions with HPMC-phthalate (HPMC-P) and PSSA acidic polymers (Figure 4)[29,30] by taking advantages of the sensitivity of ^{15}N chemical shifts to strong H-bond and protonation.[53] Comparison of the ^{15}N CP MAS NMR spectra of crystalline LB freebase, crystalline LB phthalate salt with their amorphous LB and LB-HPMC-P ASDs (Figure 4(a)) clearly show two peaks at around -350 and -335 ppm in the ASD that are attributed to the free amino N4 and protonated N4 signals, respectively. This therefore indicates the presence of acid base interaction between the protonated N4 in LB with HPMC-P, presumably via the -COO^- group and reveals for the amino (N4) signal (see grey shadow area) a significant change of chemical shift of around 17 ppm as expected between the LB phthalate salt (in which the N4 site is protonated) and freebase. While the N4 amine peak in the ^{15}N spectrum of amorphous LB appears at around -348 ppm as a single broad peak, the corresponding spectrum of the LB-HPMC-P ASDs shows the presence of two clear peak at around -350 and -355 ppm attributable respectively to the free amorphous amino N4 signal and protonated N4, as per comparison with the spectra of amorphous LB and LB phthalate salt reference sample. The existence of the protonated amine in the ASDs almost certainly means that a solid solution of the protonated LB at N4 unit in the negatively charged polymer exists. Interestingly, for the HPMC-P dispersion, the position of the N1 aniline peak does not experience any significative change. This suggest that N1 sites are not involved in any interaction and confirming that this nitrogen is not protonated in the dispersions.

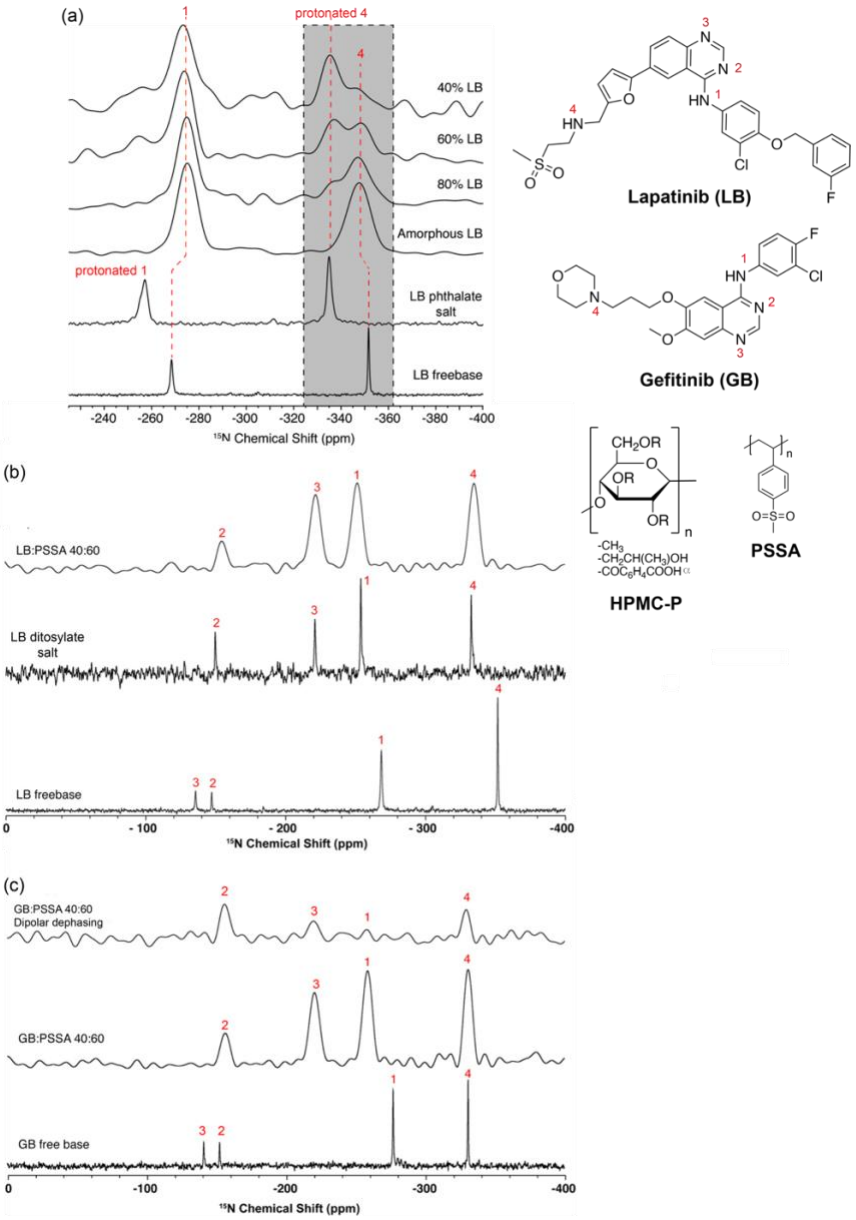

Figure 4. (a) ^{15}N CP spectra of 40, 60, 80 wt % LB-HPMC-P ASDs, amorphous LB, LB phthalate salt and freebase drug. The peak at -335 ppm in the ASD's spectrum indicates the presence of protonated amino group, hence highlighting the presence of API-polymer ionic interaction. Reprinted with permission from[29]. Copyright 2015 American Chemical Society. (b) ^{15}N CP spectra of LB freebase, LB ditosylate salt and 40 wt % LB-PSSA ASD. The large change in chemical shifts observed for N2 and N3 between the LB freebase and ASDs indicates protonation. (c) ^{15}N CP spectra of gefitinib (GB) freebase, 40 wt % LB-PSSA ASD and ^{15}N dipolar dephased spectrum of LB-PSSA ASD. Spectral assignments and chemical structures of LB, GB, HPMC-P, and PSSA are given in the figure. Reprinted with permission from[30]. Copyright 2016 American Chemical Society.

A similar approach was used to probe acid-base interactions in LB-PSSA and GB-PSSA ASDs and the corresponding ^{15}N CP MAS NMR[29,30] spectra of LB, GB, and ASDs with PSSA (Figures 4(b) and 4(c)) reveal important contribution to API-polymer interactions.[53] In both LB- and GB-PSSA ASD, the ^{15}N NMR signals of the quinazoline N sites (N3 both in LB and in GB) undergo a large shift of ~ 80 ppm to higher frequency with respect crystalline LB/GB, indicating preferential protonation of this more basic quinazoline N site. Moreover, protonation of both amine N1 and N4 signals in LB-PSSA ASD is evidenced by their similar ^{15}N shifts *vs.* LB salt confirming double protonation of the API by PSSA and strong acid-base interactions.

The presence of API-polymer interactions in the GB-PSSA ASD established above involving the quinazoline N site is not linked to a change in ^{15}N chemical shift of the ternary amine N4 (Figure 4(c)). Nevertheless, evidence of N4 being involved in the API-polymer interaction is supported by dipolar dephasing (interrupted decoupling) experiments[54] that selectively select nuclear spins strongly coupled to ^{1}H. The corresponding ^{15}N spectrum of the 40 wt % GB-PSSA ASD highlights lower signal intensity of the N1, N3, and N4 signals *vs.* N2, confirming their protonation.

Acid-base interactions have been also identified in indomethacin (IMC)-methacrylate copolymer Eudragit® E (EE) ASDs solely from ^{15}N NMR spectra[32] while overlapping ^{13}C signals between API and polymer prevented changes in chemical shifts to be observed. The ^{15}N CP MAS NMR spectra of the 20 – 60 wt % IMC-EE ASDs exhibit two peaks at around -360 ppm, attributable to the EE amino signal, and at around -344 ppm, which intensity increases with drug loading. This is further supported by some ^{15}N ^{1}H dipolar dephasing experiment carried out on the 40 % wt IMC-EE ASD that clearly shows this latter signal at -344 ppm with reduced signal intensity, indicating strong coupling to a proton, hence suggesting a protonated EE amino signal involved in the acid-base interaction with the IMC.

Hydroxypropylmethylcellulose acetyl succinate polymer (HPMC-AS) has recently been widely used to stabilise API in ASDs.[34,35,38,55,56] This is due to its unique physical-chemical properties such as high glass transition temperature (around 120 °C) and the presence of both acetyl (A) and succinoyl (S) moieties (Figure 5) which allow for effective inhibition of drug crystallization from amorphous dispersion forming hydrophobic interactions with the drug.[57,58] There is also evidence that HPMC-AS can stabilise drug in solution in *in vitro* systems and, potentially, the gastric milieu, further enhancing bioavailability of the drug by maintaining it at (or even above, at least temporarily) the saturation solubility of the drug.[59-61]

HPMC-AS was initially developed as a polymer for enteric coating of tablets, to prevent dissolution of tablets, and therefore the drug, in the stomach, or upper regions of the small intestine. Different ratios of the succinic acid (which confer pH dependent solubility) and acetic

acid groups (which hinder solubility) render the different grades of the polymer soluble at different pH ranges, with three grades available. The different ratios of these groups may be important in forming bonds and interactions with API's.

The formation of specific API-polymer interactions as it has been explored in a study in which carbamazepine (CBZ) was formulated with HPMC, HPMC-A, and HPMC-S.[33] In this work, CBZ-HPMC, CBZ-HPMC-A, and CBZ-HPMC-S were prepared by SD methodology and the API-polymer contacts were determined from multinuclear 1D NMR spectra (Figure 5).

In crystalline CBZ, the amide C1 signal resonates at 159 ppm in the spectrum and is shifted upon CBZ dispersion in HPMC, HPMC-A, and HPMC-S polymers (Figure 5(a)). These changes could confirm the amorphous behaviour of the dispersions as such changes in chemical shift between are consistent with the retention of intermolecular interactions between crystalline and amorphous specie[49], and can be used as rough indications of API-polymer interactions, that have to be confirmed by further investigations.

More interestingly, evidence of the presence of CBZ-polymer interactions in ASDs can be found by considering both the ^{1}H and ^{13}C NMR spectra shown in Figure 5(b) and (c), respectively. In contrast with the spectra of HPMC and HPMC-A polymers, the evidence of a signal at 14 ppm in the ^{1}H ultra-fast MAS (70 kHz) spectrum of 33 wt % CBZ-HPMC-S ASDs, together with the shift of the carboxyl succinoyl group C4 signal, support the presence of H-bond between CBZ and HPMC-S.[25] In a similar way, the carbonyl of the acetyl substituent C2 signal slightly shifts to lower frequencies as drug load increases, indicating the presence of H-bond between CBZ and HPMC-A.

Figure 5(d) shows the ^{1}H-^{15}N CP-based HSQC filter experiment carried out on 33 wt %^{15}N-labeled CBZ – HPMC/ HPMC-A/ HPMC-S ASDs. All ^{1}H spectra are dominated by the polymer signal at around 5.5 ppm, however an extra signal in the form of a shoulder at around 7.5 ppm is also observed for both the CBZ-HPMC-A and CBZ-HPMC-S. The presence of this signal at higher chemical shift corroborates the H-bond between the acetyl carbonyl and the CBZ's NH_2 and between both the succinoyl's carbonyls and the CBZ's NH_2 in CBZ-HPMC-A and CBZ-HPMC-S ADSs, respectively. Taking together, these results point out to the critical role that the subsistent groups A and S have in forming specific interactions with CBZ.

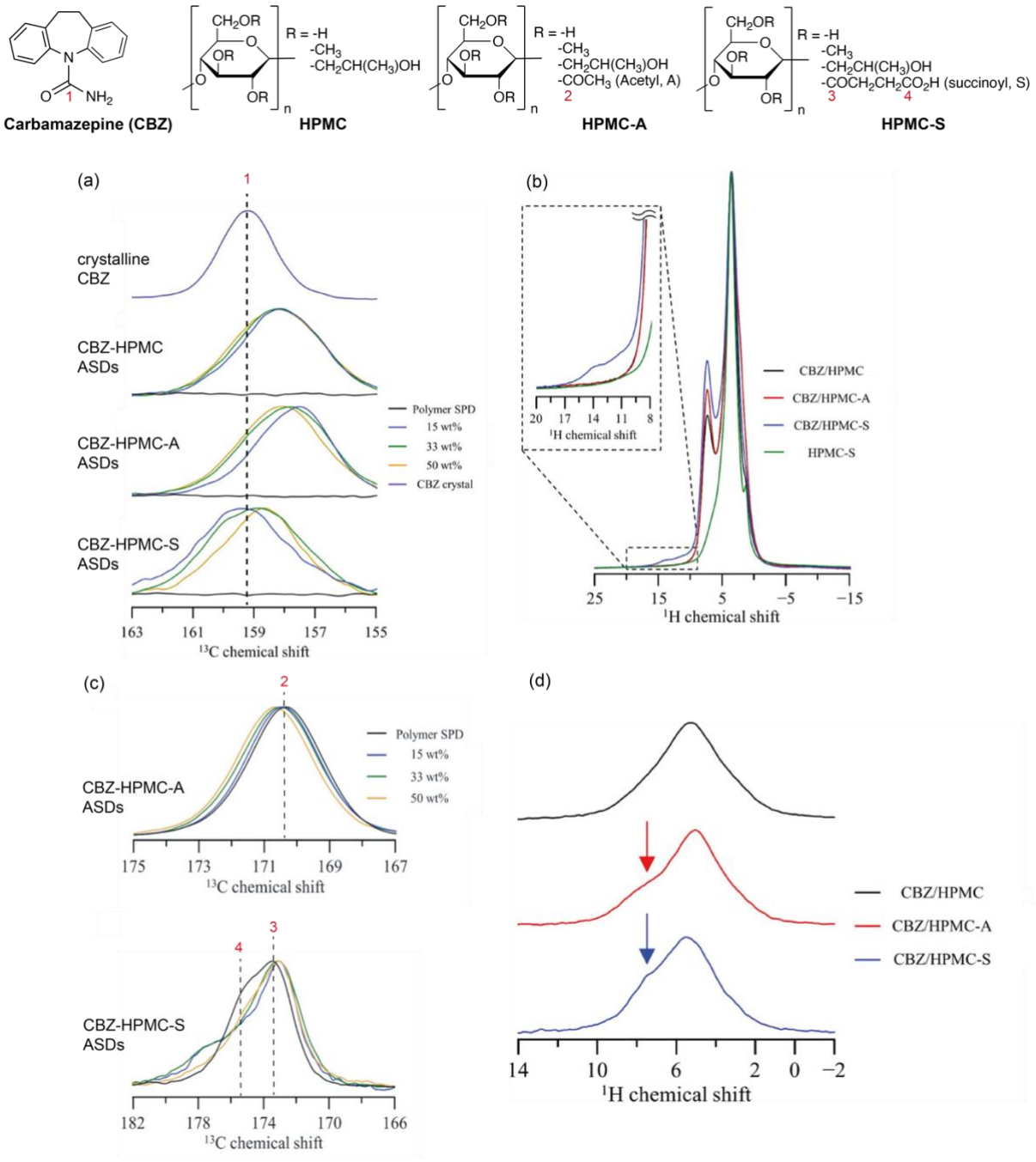

Figure 5. Magnified view of ^{13}C CP MAS NMR spectra of the (a) amide region of CBZ, (b) ^{1}H ultra-fast MAS spectra of 33 wt % CBZ-HPMC, HPMC-A, HPMC-S ASDs, and HPMC-S polymer, and (c) the carbonyls region of the polymers. (d) ^{15}N CP based HSQC filter ^{1}H MAS spectra of 33 wt % CBZ-HPMC, HPMC-A, and HPMC-S ASDs. The structure of CBZ, HPMC, HPMC-A and HPMC-S are given on the top of the figure. Reprinted with permission from[33]. Copyright 2019 American Chemical Society.

As previously reported, HPMC itself does not exhibit excellent ability of promoting the formation of H-bond with CBZ, while the use of α-Glycosyl rutin (Rutin-G), a non-polymeric

additive, brings to the formation of CBZ-Rutin-G H-bond and hence leads to significantly stabilised amorphous CBZ. This outcome is supported by both 1D NMR experiments and 2D heteronuclear correlation NMR experiment and quantum mechanical calculations.[62]

Finally, the extraordinary versatility of NMR as an evaluable toolkit in the determination of the strength and extent of H-bond has been demonstrated in an exciting work in which felodipine (FEL) API-different PVP-substituted polymers ASDs were thoroughly studied.[63] Supported by changes in ^{13}C chemical shifts and spectral intensities the degree of FEL-polymer H-bond was rank in the following ordered as PVP > (poly(vinylpyrrolidone-*co*-vinylacetate)) PVP-VA > (poly(vinylacetate)) PVAc. This result clearly indicates how the nature, strength and type of different H-bond acceptors influence the formation of effective and strong API-polymer interactions.

3. 2D correlation NMR experiments as a toolkit to probe API-polymer contacts at molecular level.

At the molecular level, the chemical species directly involved in the API-polymer interactions, as well as the observation of structural effects can be obtained from 2D NMR approaches. Together with the 1D experiments, 2D correlation experiments are well established NMR methodologies and widely used to answer critical pharmaceutical questions. They represent milestones for developing and designing advanced NMR experiments capable of increasing the range of possible information obtainable. Indeed, 2D methodologies often allow the direct detection of API–polymer contacts by correlating different nuclei, restoring spectral resolution and/or reintroducing through-space dipolar coupling interactions averaged by MAS.

In the presence of API-polymer interactions, the electronic distribution surrounding the nuclei is disturbed and changes in chemical shifts can be observed in the 1D spectra. As the atoms involved in these interactions are closed in space and interacting *via* dipolar coupling or *via* spin-diffusion, these nuclei can generate correlation signals in 2D experiments and hence are directly identified. Therefore, the evidence of the change in chemical shifts and of the presence of correlation signals in 1D and 2D experiments, respectively, together with the novel NMR methods capable of estimate interatomic distances, represent the general strategies used to understand the API-polymer interactions in ASDs. This information can be obtained in a reasonable amount of time (~ day in total for each ASD) which is an important consideration.

The HETCOR experiment has proven itself a useful technique in that respect and enables correlation spectra between heteronuclei commonly present in API (*e.g.*, usually ^{13}C but also recently ^{19}F) with the ^{1}H nucleus. The use of the ^{1}H nucleus in one of the spectral dimension

enhances the sensitivity of the experiment while the use of a heteronucleus in the other spectral dimension enhances the specificity.

An empiric estimation of the range of spin diffusion effects occurring in an HETCOR experiment can be obtained according to Equation 1, in which L, D and t are the maximum diffusion path length, spin diffusion coefficient and the time, respectively, while the brackets denote an ensemble average:

$$\langle L^2 \rangle = 6\ D\ t \qquad \text{Eq. 1}$$

The value of the spin diffusion coefficient D can be either calculated from Equation 2, in which l_0 is the distance between protons in the sample (typically in the range on 0.1 nm) and T_2 is the transverse relaxation time,[41] or found from the literature from a variety of sources on rigid and mobile polymers (D values ranging from 0.5 x 10^{-12} cm^2 s^{-1} [64] to 8.0 x 10^{-12} cm^2 s^{-1} [65] are available).

$$D = l_0^2 / T_2 \qquad \text{Eq. 2}$$

For a 500 µs contact time, Eq 1 yields an average L of about 5 Å as a maximum range over which ^{1}H-^{1}H spin diffusion can occur within the ^{1}H spin-lock period of the contact time in the CP-HETCOR experiment. Regarding the direct dipolar coupling ^{1}H-X interaction, its magnitude (transferred by the CP-HETCOR experiment) is limited to the 3-5 Å range.[12] Experimentally, it has been demonstrated that ^{19}F-^{13}C HETCOR experiments carried out at contact times of 6 ms and 8 ms can directly probe API-polymer contacts for spatially close species of 5.5 Å and 8 Å, respectively.[66]

In addition to the HETCOR experiment, methods based on the detection of homonuclear dipolar coupling, such as ^{1}H-^{1}H double quantum (DQ) correlation (for example, using the back to back (BABA) recoupling scheme[67]) have been exploited to detect API-polymer proximities in ASDs.

More recently molecular associations have been also identified via ^{14}N-^{1}H 2D experiments methodology. Despite the high natural abundance of ^{14}N (99.6 %), its low gyromagnetic ratio and large quadrupolar interaction make its direct detection in the solid state a challenge and the development of indirectly detected ^{14}N via ^{1}H, for example via 2D ^{14}N-^{1}H HMQC (Heteronuclear Multiple Quantum Coherence)[68,69] at high magnetic field (> 16.4 T) and ultra-fast MAS frequency (> 50 kHz), has enabled to solve this challenge and opened up new adventures, in particular in pharmaceutical sciences.[38,70-73]

Recent technological advancements have allowed for the development of both magnets that can handle very-high magnetic field and probes that can operate under ultra-fast MAS

condition. In particular, this latter progress has benefitted the significantly increase in resolution of ^{1}H solid-state NMR spectra by averaging out of the ^{1}H-^{1}H mononuclear dipolar interactions and opening the way to access further detailed on the structure and dynamics information in pharmaceutical formulations.[74]

Clofazimine (CLF) API - Hypromellose phthalate (HPMCS) polymer molecular interaction has been elucidated from 1D and 2D experiments.[31] Figure 6(a) shows the ^{13}C CP MAS NMR spectra of CLF-HPMC-P dispersions as a function of different API loadings. The carboxyl acid in HPMC-P (red in Figures 6(a) and (b)) and CHN in CLF (green) signals were used as spy signals to detect the presence of API-polymer interactions, and interestingly, variations in chemical shifts for both signals are observed. The changes in ^{13}C chemical shifts observed for the carboxyl acid (from around 170 ppm HPMC-P to 174.2 ppm in the dispersions) coupled to the one of the CNH in the ASD (by 2.5 ppm against the amorphous CLF) are attributed to carboxylate group bonding to CLF.

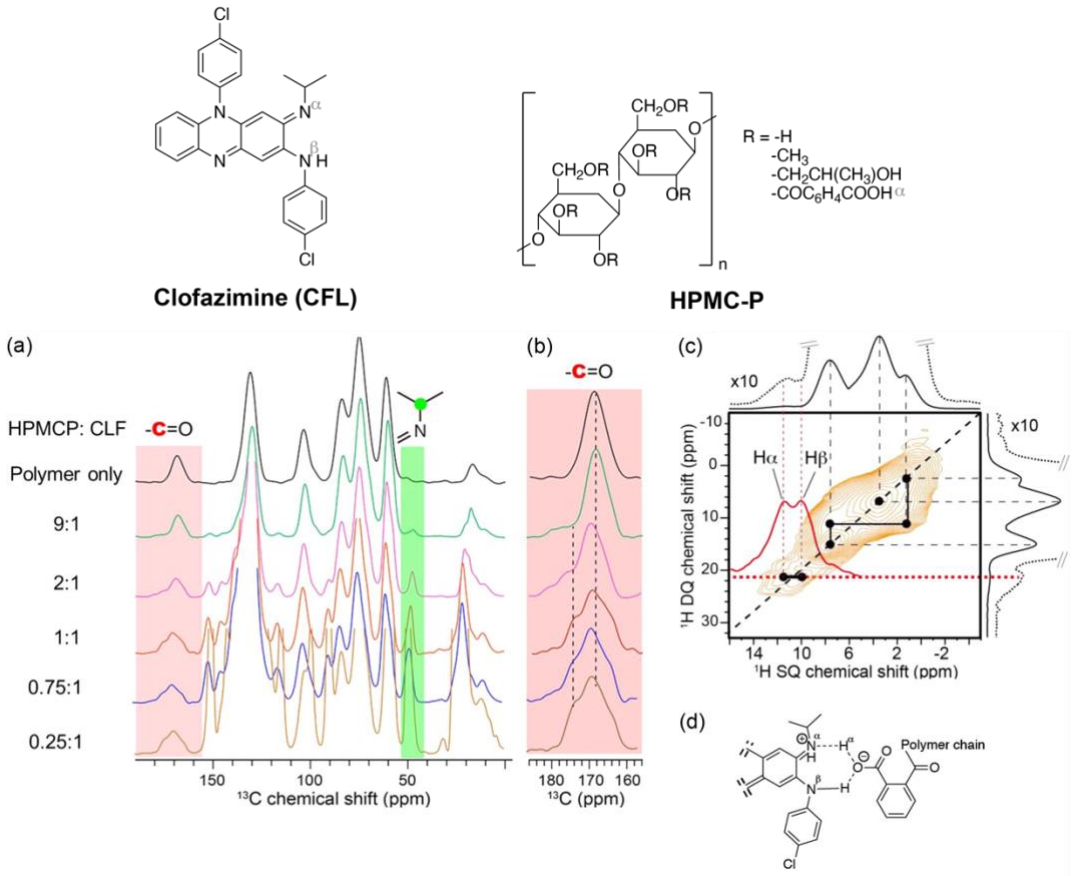

Figure 6. (a) ^{13}C CP MAS NMR spectra of CLF−HPMC-P dispersions as a function of API content. (b) Magnified view of the 157−183 ppm region. (c) ^{1}H-^{1}H DQ BABA correlation spectrum of 50 wt % CLF-HPMC-PASD exhibits a correlation between Hα and Hβ indicating the presence of carboxylate - CNH molecular interaction. The ^{1}H spectra of the CLF-HPMC-P dispersion is given on the top. (d) Schematic representation of the API-polymer interaction

via proton transfer. The chemical structures of CFL and HPMC-P are given on top. Reprinted with permission from[31]. Copyright 2016 American Chemical Society.

In order to further refine the nature of the molecular interaction occurring in this dispersion, Useful and detailed information were obtained from 2D ^{1}H-^{1}H DQ BABA experiment on the50 wt % CFL-HPMC-P ASD. The 1D ^{1}H NMR spectrum obtained under ultra-fast MAS condition of 60 kHz (top spectrum in Figure 6(c)) shows two signals at 11.5 and 10 ppm which are correlated as revealed from the 2D ^{1}H-^{1}H DQ BABA spectrum (Figure 6(c)). Interestingly, these signals have equal peak intensity (see red slice in Figure 6(c)) and their high chemical shits indicate strong H-bonding of a proton adjacent to a nitrogen atom. Considering the chemical structures of both API and polymer, these two new resonances can be assigned to the existing Nβ-Nα and the newly formed Nα-Hα contacts (see Figure 6(d)). These molecular interactions indicate a transfer proton mechanism from Hα to Nα with a concerted formation of the interaction between COO^{-} moieties with Nβ.

The capability of HPMC derivatives such as HPMC-P and HPMC-AS polymers in stabilising amorphous APIs in ASDs by forming API-polymer interactions has been also demonstrated with posaconazole (POSA, Figure 7).[34] ^{1}H-^{13}C HETCOR spectrum of 30 wt % POSA–HPMC-AS ASD (Figure 7(a)) and reveal correlated ^{13}C and ^{1}H signals at around 154 and 2 ppm, respectively, demonstrating an intermolecular H-bond interaction between the carbonyl C41 carbon of the POSA triazole ring and the HPMC-AS hydroxyl group. Another electrostatic intermolecular interaction is revealed in the HETCOR spectrum of the 30 wt % isotopically labelled ^{13}C-C44, ^{15}N-N42 and ^{15}N-N43 sites POSA in HPMC-AS ASD (Figure 7(b)) from the correlation involving ^{13}C at 136 ppm with ^{1}H at 4 ppm that indicates spatial contact of the POSA triazole ring with the -CH_2 adjacent to the carboxylic moiety in the S group. In a similar fashion, the HETCOR spectrum of 30 wt % POSA–HPMC-P ASD (Figure 7(c)) highlights two spatial proximities: an electrostatic interaction between the HPMC-S carboxylic group with the POSA triazole ring at 168 ppm/4 ppm; and a π-π aromatic stacking interaction between the HPMC-P aromatic carbons and the POSA proton attached to C46/47. These data clearly indicate the role played by the substituent groups of the HPMC backbone, as the presence of hydroxyl and carbonyl groups, triazole moieties and difluorophenyl rings favour the potential formation of strong interactions with the A and S substituents of HPMC-AS.

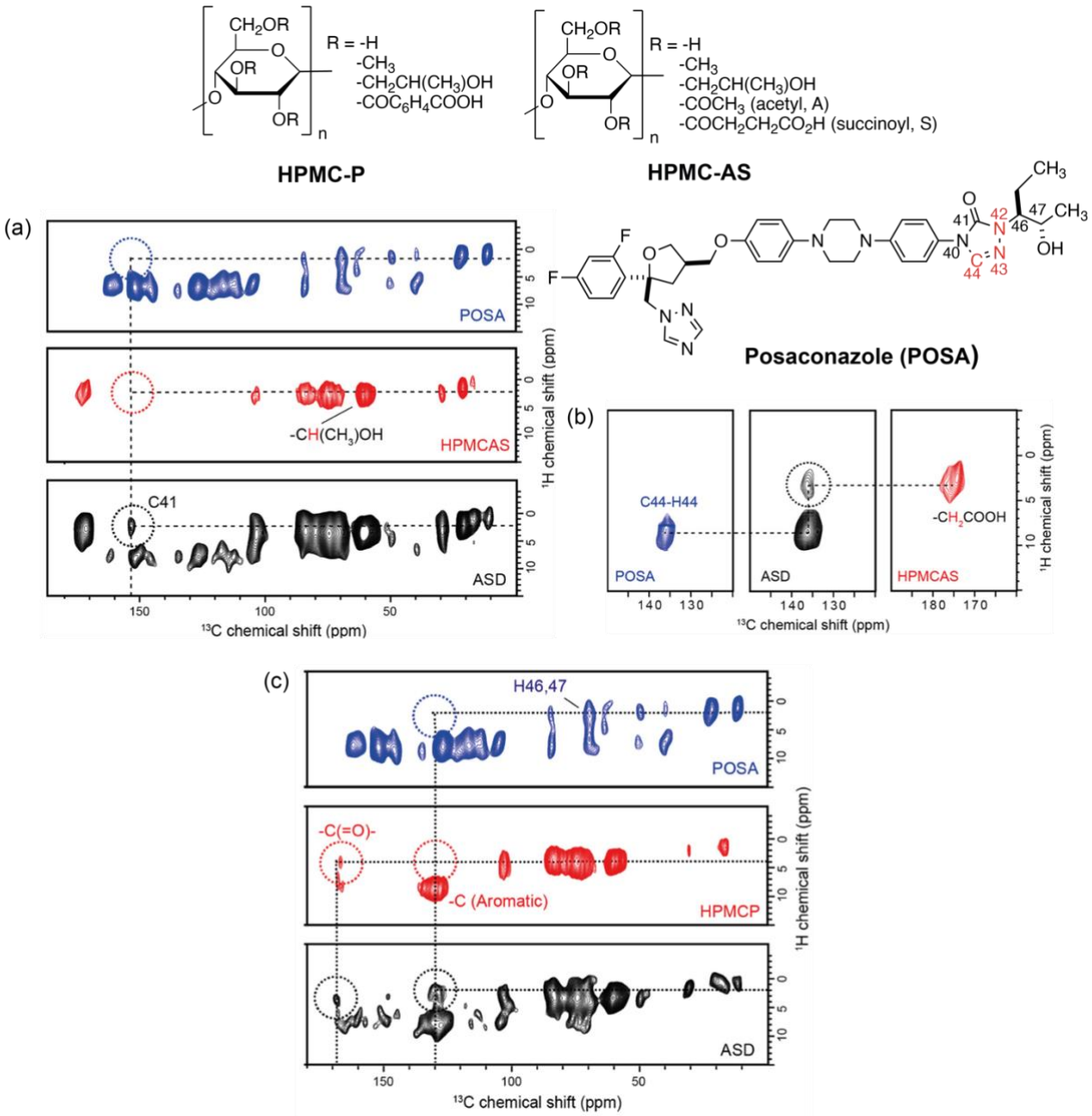

Figure 7. (a) ^{13}C CP HETCOR spectra of POSA, HPMC-AS and 30 wt % POSA–HPMC-AS ASD. (b) ^{13}C CP HETCOR spectra of isotopically labelled ^{13}C-C44, ^{15}N-N42 and ^{15}N-N43 sites POSA, as an ASD in HPMC-AS, and HPMC-AS. (c)^{13}C CP HETCOR spectra of POSA, HPMC-P and 30 wt % POSA–HPMC-AS ASD. The correlations highlighted in the black circle in all ASDs HETCOR spectra indicate the carbon signals involved in API-polymer interactions. All the spectra were carried out at a MAS frequency of 12 kHz, with a contact time of 2 ms. Chemical structures of POSA, HPMC-P and HPMC-AS are given on the bottom of the figure. Isotopically labelled C44, N42 and N43 atoms are highlighted in red. Reprinted with permission from[34]. Copyright 2019 American Chemical Society.

The presence of F atoms in the chemical structure of POSA also allows further investigation on the presence of API-polymer interactions involving these fluorinated moieties and exciting

outcomes have been reported from the characterisation of a 30 wt % POSA-HPMC-AS ASD using 2D ^{1}H-^{19}F HETCOR.[35] The corresponding spectra for crystalline and amorphous POSA (blue and red, respectively in Figure 8(a)) show similar correlations between the aromatic fluorines of the difluorophenyl group with both aromatic protons (7.5 ppm) and aliphatic protons (1.5 ppm), due to intermolecular "head-to-tail" packing. The extra correlation at around 4 ppm that appears in the HETCOR spectrum of the ASD (Figures 8(a) and 8(b)) additionally suggests the presence of an H-bond POSA-HPMC-AS interaction, likely between the hydroxyl group of HPMC-AS and the difluorophenyl group of POSA, as schematically illustrated in Figure 8(c).

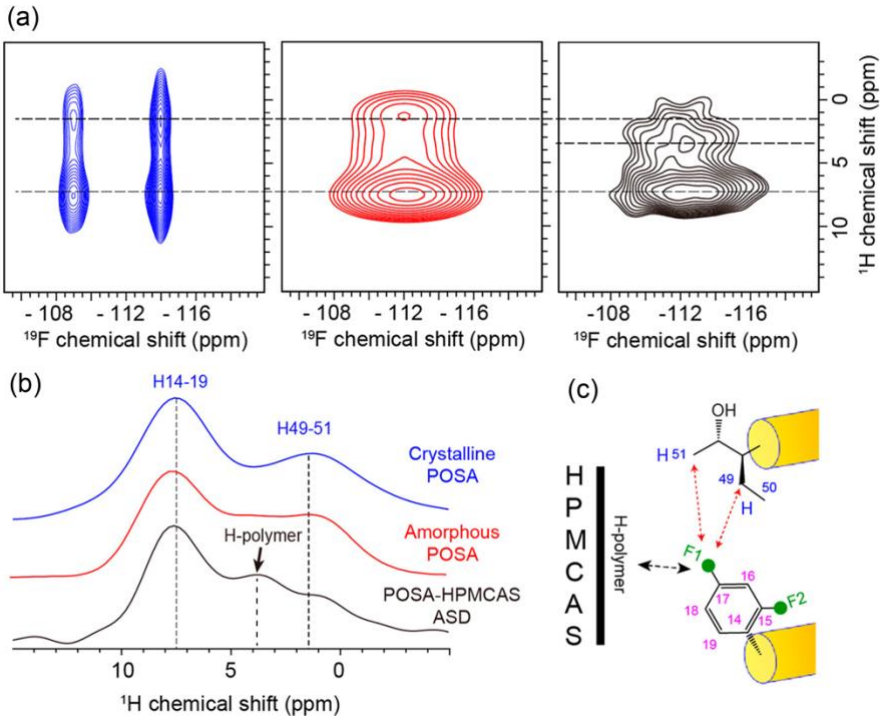

Figure 8. (a) ^{1}H-^{19}F HETCOR spectra of crystalline (blue), amorphous POSA (red), and 30 wt. % POSA–HPMC-AS ASD (black). (b) ^{1}H spectrum extracted from the HETCOR spectra at ^{19}F chemical shifts of around -114 (for crystalline POSA), -112 (for amorphous POSA), and -112 ppm (for the ASD), respectively. (c) Schematic representation of intermolecular interactions in amorphous POSA (red dashed arrows) and between POSA and HPMC-AS (black dashed arrow). Reprinted with permission from[35]. Copyright 2020 American Chemical Society.

Further understanding of the interaction in POSA-HPMC-AS ASD[35] has also been obtained from measuring fluorine-carbon interatomic distance using the well-known Rotational-Echo Double-Resonance (REDOR) experiment[75] applied to the ^{19}F-^{13}C pairs. The REDOR experiment uses rotor-synchronised radiofrequency pulses to reintroduce the MAS averaged dipolar coupling, hence allowing experimental evaluation of precise distance between heteronuclear spins. For the POSA-HPMC-AS dispersions, comparison between experimental

dephasing ^{19}F-^{13}C REDOR curves and simulation yields a close proximity of around 4.3 Å between the HPMC-AS hydroxyl group and the POSA's difluorophenyl group , adding further important details in the understanding of the POSA-HPMC-AS interaction described above.[35]

^{1}H-^{13}C and ^{1}H-^{29}Si HETCOR have been employed to identify spatial proximities and intermolecular interactions between the various components of the IMC-HPMC-mesoporous silica ternary ASD prepared using different HME screw conditions (low- and high- energy HME).[76] While the ^{1}H-^{13}C HETCOR data show proximity between IMC and HPMC, the ^{1}H-^{29}Si HETCOR spectrum provides information on the interaction between IMC-HPMC and the silicon framework. Indeed, IMC/HPMC-mesoporous silica interactions were found in the formulation prepared by the high-energy process.

A further example of the usefulness of the HETCOR technique in identifying spatial correlations between API-polymer was given in understanding the stability of structure of the abiraterone-hydroxypropyl-β-cyclodextrin dispersion[77] prepared by an innovative solvent-free technology known as KinetiSol®.[78] The ^{1}H-^{13}C HETCOR showed a clear interaction between the aromatic region of the abiraterone and the anomeric protons of the cyclodextrin.

The versatility of HPMC-AS in forming drug polymer interactions, hence stabilising ASDs has also been probed in the acetaminophen-HPMC-AS dispersions (Figure 9).[38] For the ASDs with drug loading > 20 wt %, ^{1}H-^{13}C HETCOR correlation experiments identify spatial proximities between aromatic protons of the acetaminophen with the cellulose backbone protons of the HPMC-AS polymer while the presence of H-bonds between API and polymer was established from ^{14}N-^{1}H HMQC experiments. The ^{14}N-^{1}H HMQC spectra of a 10 and 20 wt % acetaminophen-HPMC-AS ASDs (Figure 9) indicate the presence of interactions between the acetaminophen ^{14}N signal with the -OCH_3 signal (H_8) of the polymer, hence highlighting a closer contact between API and polymer that can be reasonable attributed to the presence of H-bond between this amide donor and oxygen acceptor. In contrast, the ^{14}N-^{1}H HMQC spectrum of the 40 wt % ASD exhibits correlations between the acetaminophen ^{14}N signal with all acetaminophen protons in the crystalline form, suggesting the absence of API-polymer interaction, instability, and API recrystallization with loading > 40 wt %.

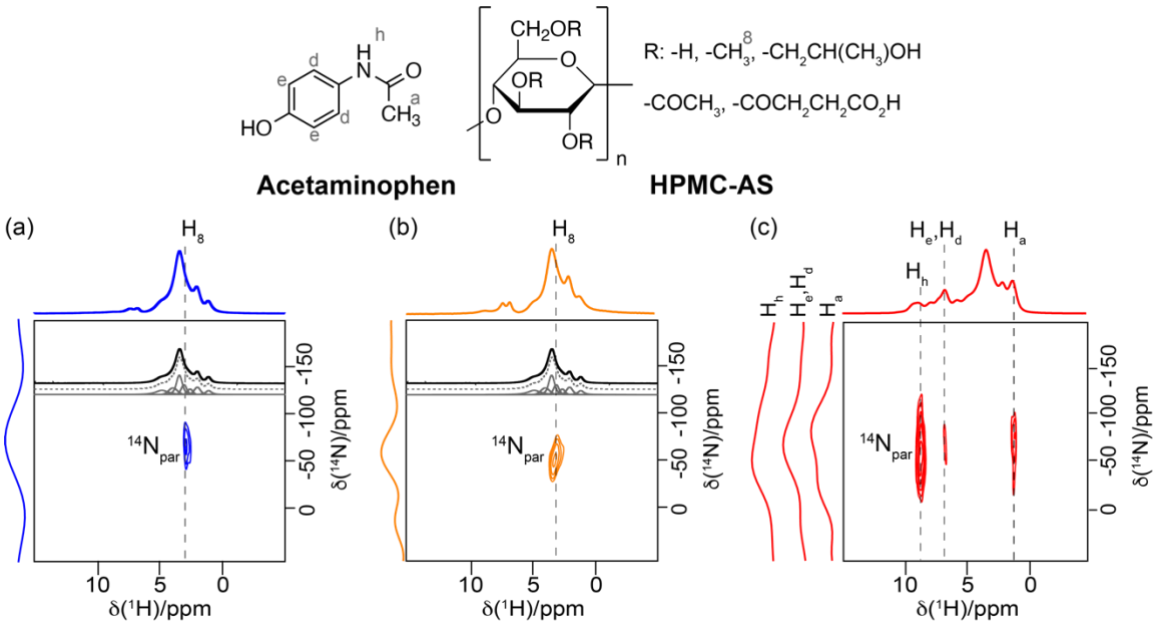

Figure 9. ^{14}N-^{1}H HMQC spectra of 10 wt % (blue), 20 wt % (orange), and 40 wt % (red) acetaminophen–HPMC-AS ASDs. The deconvoluted ^{1}H spectra of the HPMC-AS are given in black. Spectra on the left of the 2D HMQC are the ^{14}N slices extracted at the indicated ^{1}H chemical shift in dashed black lines. Chemical structures of acetaminophen and HPMC-AS are given on top. Reprinted with permission from[38]. Copyright 2021 American Chemical Society.

The evaluation and the evidence of API-polymer interactions in Rafoxanide (RAF)-PVP ASDs at drug loading of 25, 33, and 50 wt % (Figure 10), prepared via SD using two different feed solutions aqueous (a 70%:30% mixture of 0.1 M NaOH solution and acetone) and organic (80%:20% acetone/ethanol mixture), have been probed using 1D ^{13}C and ^{15}N CP experiments and further investigated carrying out 2D ^{1}H-^{1}H RFDR (radio frequency driven recoupling)[37] experiments at MAS = 110 kHz, at 18.8T (Figure 10), that leads to determine ^{1}H-^{1}H proximities by recoupling homonuclear dipolar interactions. For the 50 wt % RAF-PVP ASD made from aqueous condition, the spectrum recorded at short mixing time τ_{RFDR} of 7.2 ms (Figure 10(a)) shown correlation between the PVP aliphatic protons (2-3.5 ppm) with the RAF aromatic protons (ca. 7.5 ppm), and more importantly, exhibits long range intermolecular correlations between RAF aromatic protons and PVP aliphatic protons (peaks circled in red). Moreover, thanks to the enhanced ^{1}H resolution likely due to the benefit of very-high magnetic field together with the ultra-fast MAS condition, the enlarged RFDR spectrum (Figure 10 (c)) illustrates the presence of cross peaks between the amide ^{1}H of RAF with the aliphatic ^{1}H of PVP and highlights the expected amide – aromatic protons intramolecular correlation, indicating the presence of API-polymer intermolecular H-bond interaction involving RAF and PVP. Reasonably, the formation of this interaction is due to the aqueous feed solution used

during the SD process. In the aqueous condition, the presence of the NaOH can ionise the RAF phenolic hydroxyl group promotion the formation of H-bond between the RAF amide, as a donor, and PVP carbonyl, as an acceptor. The presence of this RAF-PVP H bond interaction for these dispersions have also been confirmed from ^{1}H-^{13}C HETCOR.[79]

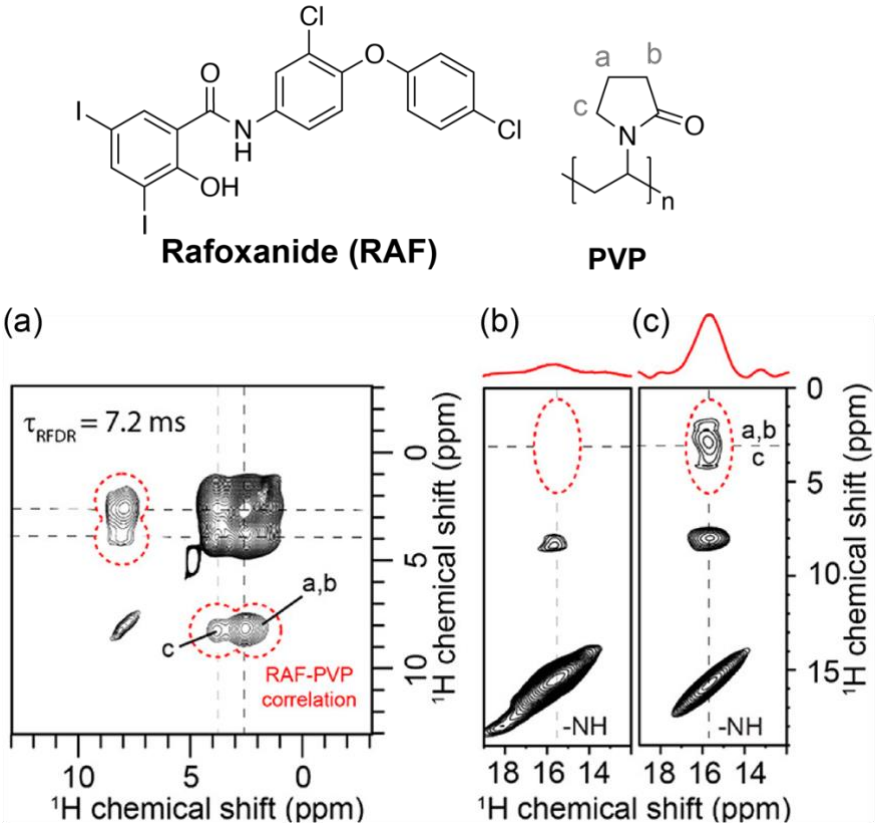

Figure 10. (a) ^{1}H-^{1}H RFDR spectra of 50 wt % RAF-PVP ASD SD from under aqueous condition carried out at mixing time τ_{RFDR} of 7.2 ms. Enlarged region of ^{1}H-^{1}H RFDR spectra carried out at (b) low and (c) very-high magnetic field, showing the evidence of the presence of RAF-PVP H-bond. Correlation peaks are highlighted with a red dot line. Chemical structure of RAF and PVP are given on top. Reprinted with permission from[37]. Copyright 2020 American Chemical Society.

4. Conclusions

In this review, we have described the latest applications of solid-state NMR spectroscopy approaches employing 1D and 2D data acquisition strategies approaches to identify and provide understanding of API-polymer interactions in pharmaceutical formulations. These studies revealed that changes of ^{1}H, ^{13}C, and ^{15}N chemical shifts in ASDs when compared with their individual components allowed the identification of API-polymer interactions such as H-bond or ionic one, while correlation spectroscopy from 2D NMR spectra has proved itself to be an excellent tool kit for molecular level identification of chemical species involved in the

API-polymer contacts, providing essential information to understanding the nature of the stabilising interactions.

Moreover, NMR methodologies can play an important role as an orthogonal approach to the various more commonly used methods such as UV, IR and XRD, in order to strengthen understanding of stability mechanism of ASDs.[28,30,31,33] Furthermore, NMR spectroscopy can be an effective and a powerful technique to aid the pharmaceutical scientist to design new potential ASDs.

Continuous development in NMR is leading to the design of increasingly sophisticated and sensitive methods and this will certainly open up opportunities to understand ASD systems, and therefore allow the rational design of appropriate systems, rather than the current empirical approach. The dynamic nuclear polarisation (DNP) technique, thanks to its enhanced sensitivity compared to traditional NMR, has been successfully applied to field of pharmaceutical sciences. Pioneering work exploring the dependence of DNP enhancement on sample composition, radical concentration, relaxation properties of the API, excipients and formulations, types of polarizing agents and proton density have been published and offer exciting perspectives.[80,81]

Author information

Corresponding Author

Frédéric Blanc – Department of Chemistry, University of Liverpool, Liverpool L69 7ZD, United Kingdom; Stephenson Institute for Renewable Energy, University of Liverpool, L69 7ZF, United Kingdom; orcid.org/0000-0001-9171-1454; email: frederic.blanc@liverpool.ac.uk

Authors

Andrea Pugliese – Department of Chemistry, University of Liverpool, Liverpool L69 7ZD, United Kingdom; orcid.org/0000-0001-7328-0670

Michael Tobyn – Drug and Product Development, Bristol-Myers Squibb, Moreton CH46 1QW, United Kingdom; orcid.org/0000-0003-0856-7821

Lucy E. Hawarden – Drug and Product Development, Bristol-Myers Squibb, Moreton CH46 1QW, United Kingdom; orcid.org/0000-0003-1718-4937

Anuji Abraham - Drug Product Development, Bristol-Myers Squibb, New Brunswick, New Jersey 08903, United States, orcid.org/0000-0003-3811-7071

Funding

A. P. thanks Bristol-Myers Squibb and the EPSRC for a PhD studentship under the scheme of the National Productivity Investment Fund (NPIF) under grant number EP/R51231X/1.

Notes

The authors declare no competing financial interest.

References

1. Edueng, K.; Mahlin, D.; Bergstrom, C. A. S. The Need for Restructuring the Disordered Science of Amorphous Drug Formulations. *Pharm. Res.* **2017,** *34,* 1754-1772.

2. Rams-Baron, M. J., R.; Boldyreva, E.; Zhou D.; Jamroz, W.; Paluch, M. , *Amorphous Drugs*. Springer, Cham, Switzerland: 2018.

3. Vasconcelos, T.; Marques, S.; das Neves, J.; Sarmento, B. Amorphous solid dispersions: Rational selection of a manufacturing process. *Adv. Drug. Deliv. Rev.* **2016,** *100,* 85-101.

4. Davis, M.; Walker, G. Recent Strategies in Spray Drying for the enhanced bioavailability of poorly water-soluble drugs. *J. Control Release* **2018,** *269,* 110-127.

5. Bhujbal, S. V.; Mitra, B.; Jain, U.; Gong, Y.; Agrawal, A.; Karki, S.; Taylor, L. S.; Kumar, S.; Tony Zhou, Q. Pharmaceutical amorphous solid dispersion: A review of manufacturing strategies. *Acta. Pharm. Sin. B* **2021,** *11,* 2505-2536.

6. Baghel, S.; Cathcart, H.; O'Reilly, N. J. Polymeric Amorphous Solid Dispersions: A Review of Amorphization, Crystallization, Stabilization, Solid-State Characterization, and Aqueous Solubilization of Biopharmaceutical Classification System Class II Drugs. *J .Pharm. Sci.* **2016,** *105,* 2527-2544.

7. Singh, A.; Van den Mooter, G. Spray drying formulation of amorphous solid dispersions. *Adv. Drug. Deliv. Rev.* **2016,** *100,* 27-50.

8. Newman, A., *Pharmaceutical Amorphous Solid Dispersions*. Wiley, Hobken, New Jersey, USA: 2015.

9. Van Duong, T.; Van den Mooter, G. The role of the carrier in the formulation of pharmaceutical solid dispersions. Part II: amorphous carriers. *Expert. Opin. Drug. Deliv.* **2016,** *13,* 1681-1694.

10. Wang, Y.; Wang, Y.; Cheng, J.; Chen, H.; Xu, J.; Liu, Z.; Shi, Q.; Zhang, C. Recent Advances in the Application of Characterization Techniques for Studying Physical Stability of Amorphous Pharmaceutical Solids. *Crystals* **2021,** *11,* 1440-1458.

11. Van den Mooter, G.; Van den Brande, J.; Augustijns, P.; Kinget, R. Glass Forming Properties of Benzodiazepines and Co-evaporate Systems with Poly(hydroxyethyl Methacrylate). *J. Therm. Anal. Calorim.* **1999,** *57,* 493-507.

12. Pham, T. N.; Watson, S. A.; Edwards, A. J.; Chavda, M.; Clawson, J. S.; Strohmeir, M.; Vogt, F. G. Analysis of Amorphous Solid Dispersions Using 2D Solid-State NMR and 1H T1 Relaxation Measurements. *Mol. Pharmaceutics* **2010,** *7,* 1667-1691.

13. Gordon, M.; Taylor, J. S. Ideal Copolymers and the Second-Order Transition of Synthetic Rubbers. I. Non crystalline Copolymers. *Rubber Chem. Technol.* **1953,** *26,* 323-335.

14. Tobyn, M.; Brown, J.; Dennis, A. B.; Fakes, M.; Gao, Q.; Gamble, J.; Khimyak, Y. Z.; McGeorge, G.; Patel, C.; Sinclair, W.; Timmins, P.; Yin, S. Amorphous drug-PVP dispersions: application of theoretical, thermal and spectroscopic analytical techniques to the study of a molecule with intermolecular bonds in both the crystalline and pure amorphous state. *J. Pharm. Sci.* **2009,** *98,* 3456-3468.

15. McNamara, D.; Yin, S.; Pan, D.; Crull, G.; Timmins, P.; Vig, B. Characterization of Phase Separation Propensity for Amorphous Spray Dried Dispersions. *Mol. Pharmaceutics* **2017,** *14,* 377-385.

16. Furuyama, N.; Hasegawa, S.; Hamaura, T.; Yada, S.; Nakagami, H.; Yonemochi, E.; Terada, K. Evaluation of solid dispersions on a molecular level by the Raman mapping technique. *Int. J. Pharm.* **2008,** *361,* 12-18.

17. Breitenbach, J.; Schrof, W.; Neumann, J. Confocal Raman-Spectroscopy: Analytical Approach to Solid Dispersions and Mapping of Drugs. *Mol. Pharm.* **1999,** *16,* 1109-1113.

18. Taylor, L. S.; Zografi, G. Spectroscopic Characterization of Interactions Between PVP and Indomethacin in Amorphous Molecular Dispersions. *Pharm. Res.* **1997,** *14,* 1691-1698.

19. Tran, T. T. D.; Tran, P. H. L. Molecular Interactions in Solid Dispersions of Poorly Water-Soluble Drugs. *Pharmaceutics* **2020,** *12,* 745-757.

20. Laws, D. D.; Bitter, H. L.; Jerschow, A. Solid-State NMR Spectroscopic Methods in Chemistry. *Angew. Chem. Int. Ed.* **2002,** *41,* 3096-3129.

21. Reif, B.; Ashbrook, S. E.; Emsley, L.; Hong, M. Solid-state NMR spectroscopy. *Nat. Rev. Methods Primers* **2021,** *1,* 1-23.

22. Everett, J. R.; Harris, R. K.; Lindon, J. C., *NMR in Pharmaceutical Sciences*. John Wiley & Sons: Chichester, UK, 2015.

23. Holzgrabe, U.; Wawer, I.; Diehl, B., *NMR spectroscopy in Pharmaceutical Analysis*. Elsevier Science: Oxford, 2008.

24. Pellecchia, M.; Bertini, I.; Cowburn, D.; Dalvit, C.; Giralt, E.; Jahnke, W.; James, T. L.; Homans, S. W.; Luchinat, C.; Meyer, B.; Oschkinat, H.; Peng, J.; Schwalbe, H.; Siegal, G.

Perspectives on NMR in drug discovery: a technique comes of age *Nat. Rev. Drug Discov.* **2008,** *7,* 738-745.

25. Pugliese, A.; Hawarden, L. E.; Abraham, A.; Tobyn, M.; Blanc, F. Solid State Nuclear Magnetic Resonance Studies of Hydroxypropylmethylcellulose Acetyl Succinate Polymer, a Useful Carrier in Pharmaceutical Solid Dispersions. *Magn. Reson. Chem.* **2020,** *58,* 1036-1048.

26. Pisklak, D. M.; Zielinska-Pisklak, M.; Szeleszczuk, L.; Wawer, I. ^{13}C solid-state NMR analysis of the most common pharmaceutical excipients used in solid drug formulations Part II: CP kinetics and relaxation analysis. *J. Pharm. Biomed. Anal.* **2016,** *122,* 29-34.

27. Harris, R. K. Applications of solid-state NMR to pharmaceutical polymorphism and related matters. *J Pharm Pharmacol* **2007,** *59,* 225-239.

28. Mistry, P.; Mohapatra, S.; Gopinath, T.; Vogt, F. G.; Suryanarayanan, R. Role of the Strength of Drug-Polymer Interactions on the Molecular Mobility and Crystallization Inhibition in Ketoconazole Solid Dispersions. *Mol. Pharmaceutics* **2015,** *12,* 3339-3350.

29. Song, Y.; Yang, X.; Chen, X.; Nie, H.; Byrn, S.; Lubach, J. W. Investigation of Drug-Excipient Interactions in Lapatinib Amorphous Solid Dispersions Using Solid-State NMR Spectroscopy. *Mol. Pharmaceutics* **2015,** *12,* 857-866.

30. Song, Y.; Zemlyanov, D.; Chen, X.; Nie, H.; Su, Z.; Fang, K.; Yang, X.; Smith, D.; Byrn, S.; Lubach, J. W. Acid-Base Interactions of Polystyrene Sulfonic Acid in Amorphous Solid Dispersions Using a Combined UV/FTIR/XPS/ssNMR Study. *Mol. Pharmaceutics* **2016,** *13,* 483-492.

31. Nie, H.; Su, Y.; Zhang, M.; Song, Y.; Leone, A.; Taylor, L. S.; Marsac, P. J.; Li, T.; Byrn, S. R. Solid-State Spectroscopic Investigation of Molecular Interactions between Clofazimine and Hypromellose Phthalate in Amorphous Solid Dispersions. *Mol. Pharmaceutics* **2016,** *13,* 3964-3975.

32. Lubach, J. W.; Hau, J. Solid-State NMR Investigation of Drug-Excipient Interactions and Phase Behavior in Indomethacin-Eudragit E Amorphous Solid Dispersions. *Pharm. Res.* **2018,** *35,* 65.

33. Ishizuka, Y.; Ueda, K.; Okada, H.; Takeda, J.; Karashima, M.; Yazawa, K.; Higashi, K.; Kawakami, K.; Ikeda, Y.; Moribe, K. Effect of Drug-Polymer Interactions through Hypromellose Acetate Succinate Substituents on the Physical Stability on Solid Dispersions Studied by Fourier-Transform Infrared and Solid-State Nuclear Magnetic Resonance. *Mol. Pharmaceutics* **2019,** *16,* 2785-2794.

34. Lu, X.; Huang, C.; Lowinger, M. B.; Yang, F.; Xu, W.; Brown, C. D.; Hesk, D.; Koynov, A.; Schenck, L.; Su, Y. Molecular Interactions in Posaconazole Amorphous Solid Dispersions from Two-Dimensional Solid-State NMR Spectroscopy. *Mol. Pharmaceutics* **2019,** *16,* 2579-2589.

35. Lu, X.; Li, M.; Huang, C.; Lowinger, M. B.; Xu, W.; Yu, L.; Byrn, S. R.; Templeton, A. C.; Su, Y. Atomic-Level Drug Substance and Polymer Interaction in Posaconazole Amorphous Solid Dispersion from Solid-State NMR. *Mol. Pharmaceutics* **2020,** *17,* 2585-2598.

36. Lu, X.; Huang, C.; Li, M.; Skomski, D.; Xu, W.; Yu, L.; Byrn, S. R.; Templeton, A. C.; Su, Y. Molecular Mechanism of Crystalline-to-Amorphous Conversion of Pharmaceutical Solids from (19)F Magic Angle Spinning NMR. *J. Phys. Chem. B* **2020,** *124,* 5271-5283.

37. Li, M.; Meng, F.; Tsutsumi, Y.; Amoureux, J. P.; Xu, W.; Lu, X.; Zhang, F.; Su, Y. Understanding Molecular Interactions in Rafoxanide-Povidone Amorphous Solid Dispersions from Ultrafast Magic Angle Spinning NMR. *Mol. Pharmaceutics* **2020,** *17,* 2196-2207.

38. Pugliese, A.; Toresco, M.; McNamara, D.; Iuga, D.; Abraham, A.; Tobyn, M.; Hawarden, L. E.; Blanc, F. Drug-Polymer Interactions in Acetaminophen/Hydroxypropylmethylcellulose Acetyl Succinate Amorphous Solid Dispersions Revealed by Multidimensional Multinuclear Solid-State NMR Spectroscopy. *Mol. Pharmaceutics* **2021,** *18,* 3519-3531.

39. Paudel, A.; Geppi, M.; Van den Mooter, G. Structural And Dynamic Properties of Amorphous Solid Dispersions: The Role of Solid-State Nuclear Magnetic Resonance Spectroscopy and Relaxometry. *J. Pharm. Sci.* **2014,** *103,* 2635-2662.

40. Li, M.; Xu, W.; Su, Y. Solid-State NMR Spectroscopy in Pharmaceutical Sciences. *TrAC Trends in Analytical Chemistry* **2021,** 116152.

41. Marchetti, A.; Yin, J.; Su, Y.; Kong, X. Solid-State NMR in the Field of Drug Delivery: State of the Art and New Perspectives. *Magnetic Resonance Letters* **2021,** *1,* 28-70.

42. Du, Y.; Su, Y. ^{19}F Solid-State NMR Characterization of Pharmaceutical Solids. *Solid State Nucl. Magn. Reson.* **2022,** *120,* 101796.

43. Levitt, M. H., *Spin Dynamics*. 2nd ed.; Wiley, West Sussex, England: 2008.

44. Keeler, J., *Understanding NMR Spectroscopy*. 2nd ed.; Wiley, West Sussex, England: 2010.

45. Gunther, H., *NMR Spectroscopy: Basic Principles, Concepts, and Applications in Chemistry*. 3rd ed.; Wiley, Weinheim, Germany: 2013.

46. Hore, P. J., *Nuclear Magnetic Resonance*. 2nd ed.; Oxford press, Oxford, England: 2015.

47. Duer, M., *Introduction to Solid-State NMR Spectroscopy*. Blackwell Publishing, Oxford, England: 2005.

48. Apperley, D. C.; Harris, R. K.; Hodgkinson, P., *Solid-State NMR: Basic Principle & Practice*. Momentum Press, New York, USA: 2012.

49. Lu, X.; Xu, W.; Hanada, M.; Jermain, S. V.; Williams, R. O., 3rd; Su, Y. Solid-state NMR analysis of crystalline and amorphous Indomethacin: An experimental protocol for full resonance assignments. *J. Pharm. Biomed. Anal.* **2019,** *165,* 47-55.

50. Schuster, I. I.; Roberts, J. D. Nitrogen-15 nuclear magnetic resonance spectroscopy. Effects of hydrogen bonding and protonation on nitrogen chemical shift in imidazoles. *J. Org. Chem.* **1979,** *44,* 3864-3867.

51. Sarpal, K.; Tower, C. W.; Munson, E. J. Investigation into Intermolecular Interactions and Phase Behavior of Binary and Ternary Amorphous Solid Dispersions of Ketoconazole. *Mol. Pharmaceutics* **2020,** *17,* 787-801.

52. Van Eerdenbrugh, B.; Taylor, L. S. An ab initio polymer selection methodology to prevent crystallization in amorphous solid dispersions by application of crystal engineering principles. *CrystEngComm* **2011,** *13,* 6171-6178.

53. Li, Z. J.; Abramov, Y.; Bordner, J.; Jason Leonard; Medek, A.; Trask, A. V. Solid-State Acid-Base Interactions in Complexes of Heterocyclic Bases with Dicarboxylic Acids: Crystallography, Hydrogen Bond Analysis, and 15N NMR Spectroscopy. *J. Am. Chem. Soc.* **2006,** *128,* 8199-8210.

54. Smernik, R. J.; O'ades, J. M., K. Solid-state ^{13}C-NMR dipolar dephasing experiments for quantifying protonated and non-protonated carbon in soil organic matter and model systems. *European Journal of Soil Science* **2001,** *52,* 103-120.

55. Demuth, B.; Galata, D. L.; Balogh, A.; Szabo, E.; Nagy, B.; Farkas, A.; Hirsch, E.; Pataki, H.; Vigh, T.; Mensch, J.; Verreck, G.; Nagy, Z. K.; Marosi, G. Application of hydroxypropyl methylcellulose as a protective agent against magnesium stearate induced crystallization of amorphous itraconazole. *Eur. J. Pharm. Sci.* **2018,** *121,* 301-308.

56. Monschke, M.; Wagner, K. G. Impact of HPMCAS on the Dissolution Performance of Polyvinyl Alcohol Celecoxib Amorphous Solid Dispersions. *Pharmaceutics* **2020,** *12,* 541-558.

57. Friesen, D. T.; Shanker, R.; Crew, M.; Smithey, D. T.; Curatolo, W. J.; Nightingale, J. A. S. Hydroxypropyl Methylcellulose Acetate Succinate-Based Spray-Dried Dispersions: An Overview. *Mol. Pharmaceutics* **2008,** *5,* 1003-1019.

58. Sarabu, S.; Kallakunta, V. R.; Bandari, S.; Batra, A.; Bi, V.; Durig, T.; Zhang, F.; Repka, M. A. Hypromellose acetate succinate based amorphous solid dispersions via hot melt extrusion: Effect of drug physicochemical properties. *Carbohydr. Polym.* **2020,** *233,* 115828.

59. Indulkar, A. S.; Box, K. J.; Taylor, R.; Ruiz, R.; Taylor, L. S. pH-Dependent Liquid-Liquid Phase Separation of Highly Supersaturated Solutions of Weakly Basic Drugs. *Mol. Pharmaceutics* **2015,** *12,* 2365-77.

60. Taylor, L. S.; Zhang, G. G. Z. Physical chemistry of supersaturated solutions and implications for oral absorption. *Adv. Drug Deliv. Rev.* **2016,** *101,* 122-142.

61. Newman, A.; Hastedt, J. E.; Yazdanian, M. New directions in pharmaceutical amorphous materials and amorphous solid dispersions, a tribute to Professor George Zografi – Proceedings of the June 2016 Land O'Lakes Conference. *AAPS Open* **2017,** *3*.

62. Aoki, C.; Ma, X.; Higashi, K.; Ishizuka, Y.; Ueda, K.; Kadota, K.; Fukuzawa, K.; Tozuka, Y.; Kawakami, K.; Yonemochi, E.; Moribe, K. Stabilization mechanism of amorphous carbamazepine by transglycosylated rutin, a non-polymeric amorphous additive with a high glass transition temperature. *Int. J. Pharm.* **2021,** *600,* 120491.

63. Sarpal, K.; Delaney, S.; Zhang, G. G. Z.; Munson, E. J. Phase Behavior of Amorphous Solid Dispersions of Felodipine: Homogeneity and Drug-Polymer Interactions. *Mol. Pharmaceutics* **2019,** *16,* 4836-4851.

64. Spiegel, S.; Schmidt-Rohr, K.; Boeffel, C.; Spiess, H. W. ^{1}H Spin Diffusion Coefficients of Highly Mobile Polymers. *Polymers* **1993,** *34,* 4566–4569.

65. Clauss, J.; Schmidt-Rohr, K.; Spiess, H. W. Determination of Domain Sizes in Heterogeneous Polymers by Solid-State NMR. *Acta Polym.* **1993,** *44,* 1-17.

66. Abraham, A.; Crull, G. Understanding API-Polymer Proximities in Amorphous Stabilized Composite Drug Products Using Fluorine-Carbon 2D HETCOR Solid-State NMR. *Mol. Pharmaceutics* **2014,** *11,* 3754-3759.

67. Feike, M.; Demco, D. E.; Graf, R.; Gottwald, J.; Hafner, S.; Spiess, H. W. Broadband Multiple-Quantum NMR spectroscopy. *J. Magn. Reson., Ser. A* **1996,** *122,* 214-221.

68. Gan, Z.; Amoureux, J. P.; Trébosc, J. Proton-Detected ^{14}N MAS NMR Using Homonuclear Decoupled Rotary Resonance. *Chem. Phys. Lett.* **2007,** *435,* 163-169.

69. Tatton, A. S.; Bradley, J. P.; Iuga, D.; Brown, S. P. $^{14}N–^{1}H$ Heteronuclear Multiple-Quantum Correlation Magic-Angle Spinning NMR Spectroscopy of Organic Solids. *Z. Phys. Chem.* **2012,** *226,* 1187-1203.

70. Tatton, A. S.; Pham, T. N.; Vogt, F. G.; Iuga, D.; Edwards, A. J.; Brown, S. P. Probing intermolecular interactions and nitrogen protonation in pharmaceuticals by novel ^{15}N-edited and 2D ^{14}N-^{1}H solid-state NMR. *CrystEngComm* **2012,** *14,* 2654-2659.

71. Maruyoshi, K.; Iuga, D.; Antzutkin, O. N.; Alhalaweh, A.; Velaga, S. P.; Brown, S. P. Identifying the intermolecular hydrogen-bonding supramolecular synthons in an indomethacin-nicotinamide cocrystal by solid-state NMR. *ChemCommun* **2012,** *48,* 10844-10846.

72. Tatton, A. S.; Pham, T. N.; Vogt, F. G.; Iuga, D.; Edwards, A. J.; Brown, S. P. Probing hydrogen bonding in cocrystals and amorphous dispersions using ^{14}N-^{1}H HMQC solid-state NMR. *Mol. Pharmaceutics* **2013,** *10,* 999-1007.

73. Grune, M.; Luxenhofer, R.; Iuga, D.; Brown, S. P.; Poppler, A. C. ^{14}N-^{1}H HMQC solid-state NMR as a powerful tool to study amorphous formulations - an exemplary study of paclitaxel loaded polymer micelles. *J. Mater. Chem. B* **2020,** *8,* 6827-6836.

74. Quinn, C. M.; Wang, M.; Polenova, T. NMR of Macromolecular Assemblies and Machines at 1 GHz and Beyond: New Transformative Opportunities for Molecular Structural Biology. *Methods Mol. Biol.* **2018,** *1688,* 1-35.

75. Gullion, T.; Schaefer, J. Rotational-Echo Doube-Resonance NMR. *J. Magn. Reson.* **1989,** *81,* 196-200.

76. Hanada, M.; Jermain, S. V.; Lu, X.; Su, Y.; Williams, R. O., 3rd. Predicting Physical Stability of Ternary Amorphous Solid Dispersions Using Specific Mechanical Energy in a Hot Melt Extrusion Process. *Int. J. Pharm.* **2018,** *548,* 571-585.

77. Gala, U. H.; Miller, D. A.; Su, Y.; Spangenberg, A.; Williams, R. O. B., 3rd. The Effect of Drug Loading on the Properties of Abiraterone-Hydroxypropyl Beta Cyclodextrin Solid Dispersions Processed by Solvent Free KinetiSol(R) Technology. *Eur. J. Pharm. Biopharm.* **2021,** *165,* 52-65.

78. Ellenberger, D. J.; Miller, D. A.; Williams, R. O., 3rd. Expanding the Application and Formulation Space of Amorphous Solid Dispersions with KinetiSol$^{(R)}$: a Review. *AAPS PharmSciTech* **2018,** *19,* 1933-1956.

79. Meng, F.; Ferreira, R.; Su, Y.; Zhang, F. A Novel Amorphous Solid Dispersion Based on Drug-Polymer Complexation. *Drug. Deliv. Transl. Res.* **2021,** *11,* 2072-2084.

80. Ni, Q. Z.; Yang, F.; Can, T. V.; Sergeyev, I. V.; D'Addio, S. M.; Jawla, S. K.; Li, Y.; Lipert, M. P.; Xu, W.; Williamson, R. T.; Leone, A.; Griffin, R. G.; Su, Y. In Situ Characterization of Pharmaceutical Formulations by Dynamic Nuclear Polarization Enhanced MAS NMR. *J. Phys. Chem. B* **2017,** *121,* 8132-8141.

81. Zhao, L.; Pinon, A. C.; Emsley, L.; Rossini, A. J. DNP-enhanced solid-state NMR spectroscopy of active pharmaceutical ingredients. *Magn. Reson. Chem.* **2018,** *56,* 583-609.